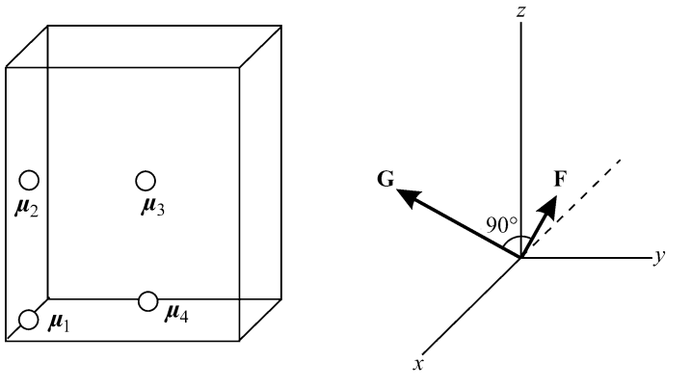

Fig. 1.5.6.1. Schematic representation of the rotation of the vectors **G** and **F** (in the xz plane) at a reorientation transition in orthoferrites.

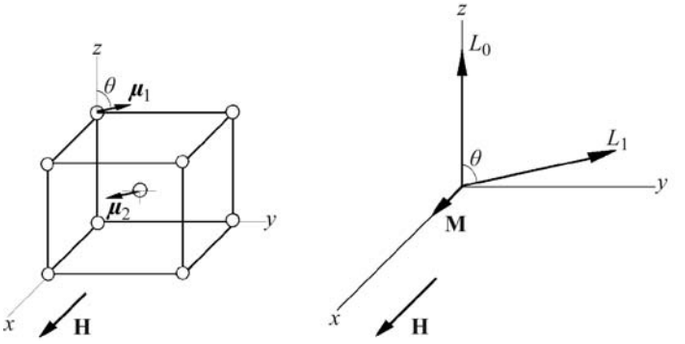

Fig. 1.5.6.2. Schematic representation of the rotation of the vector **L** under the action of a magnetic field applied to CoF_2 perpendicular to the fourfold axis z (reorientation transition) (see Figs. 1.5.5.3*a* and *b*).

There is the following change in the magnetic space groups at this transition:

$$R\bar{3}c' \overset{T_M}{\longleftrightarrow} \begin{cases} P2/c & (1.5.6.3) \\ P2'/c' & (1.5.6.4) \end{cases}$$

Which of the two groups is realized at high temperatures depends on the sign of the anisotropy constant $K'_\perp$ in equation (1.5.3.9). Neither of the high-temperature magnetic space groups is a subgroup of the low-temperature group. Therefore the transition under consideration cannot be a second-order transition.

Reorientation transitions have been observed in many orthoferrites and orthochromites. Orthoferrites of Ho, Er, Tm, Nd, Sm and Dy possess the structure $\boldsymbol{G}_x\boldsymbol{F}_z$ [see (1.5.5.8)] at room temperature. The first five of them undergo reorientation transitions to the structure $\boldsymbol{G}_z\boldsymbol{F}_x$ at lower temperatures. This reorientation occurs gradually, as in Co. Both vectors **L** and $\mathbf{M}_D$ rotate simultaneously, as shown in Fig. 1.5.6.1. These vectors remain perpendicular to each other, but the value of $\mathbf{M}_D$ varies from $(d_1/B)L$ for M_{Dz} to $(d_2/B)L$ for M_{Dx}. The coefficients d_1 and d_2 belong to the terms L_xM_z and L_zM_x, respectively. The following magnetic point groups are observed when these transitions occur:

$$\frac{2'_x}{m'_x}\frac{2'_y}{m'_y}\frac{2_z}{m_z} \overset{T_1}{\longleftrightarrow} \frac{2'_y}{m'_y} \overset{T_2}{\longleftrightarrow} \frac{2_x}{m_x}\frac{2'_y}{m'_y}\frac{2'_z}{m'_z}. \qquad (1.5.6.5)$$

Anomalies typical for second-order transitions were observed at the temperatures T_1 and T_2. The interval $T_2 - T_1$ varies from 10 to 100 K.

At low temperatures, $DyFeO_3$ is an easy-axis antiferromagnet without weak ferromagnetism – $\boldsymbol{G}_y$. It belongs to the trivial magnetic point group $\boldsymbol{D}_{2h} = mmm$. At T_M = 40 K, $DyFeO_3$ transforms into a weak ferromagnet $\boldsymbol{G}_x\boldsymbol{F}_z$. This is a first-order reorientation transition of the type

$$\boldsymbol{D}_{2h} = mmm \overset{T_M}{\longleftrightarrow} \boldsymbol{D}_{2h}(\boldsymbol{C}_{2h}) = m'm'm. \qquad (1.5.6.6)$$

Reorientation transitions in antiferromagnets occur not only as a result of a sign change of the anisotropy constant. They can be governed by the applied magnetic field. In Section 1.5.3.3.2, we described the spin-flop first-order reorientation transition in an easy-axis antiferromagnet. This transition splits into two second-order transitions if the magnetic field is not strictly parallel to the axis of the crystal. There is a specific type of reorientation transition, which occurs in antiferromagnets that do not exhibit weak ferromagnetism, but would become weak ferromagnets if the antiferromagnetic vector was directed along another crystallographic direction. As an example, let us consider such a transition in CoF_2. It is a tetragonal crystal with crystallographic space group $\boldsymbol{D}_{4h}^{14} = P4_2/mnm$. Below T_N, CoF_2 becomes an easy-axis antiferromagnet. The magnetic structure of this crystal is shown in Fig. 1.5.5.3. Its magnetic point group is $\boldsymbol{D}_{4h}(\boldsymbol{D}_{2h}) = 4'/mmm'$. Let us apply the magnetic field H parallel to the twofold axis x (see Fig. 1.5.6.2). In a typical antiferromagnet, the field stimulates a magnetization $M = \chi_\perp H$. The structure $\boldsymbol{D}_{4h}^{14} = P4_2/mnm$ allows weak ferromagnetism if **L** is perpendicular to the z axis. As a result, if the vector **L** is deflected from the z axis by an angle θ in the plane yz perpendicular to the x axis, the magnetization will rise according to the relation

$$M = \chi_\perp(H + H_D \sin\theta), \qquad (1.5.6.7)$$

where $H_D = M_D/\chi_\perp$ [see (1.5.5.3) and (1.5.5.4)]. As a result, there is a gain in the magnetic energy, which compensates the loss in the anisotropy energy. The beginning of the deflection is a second-order transition. The balance of both energies determines the value of θ:

$$\sin\theta = (H_e/H_aH_D)H. \qquad (1.5.6.8)$$

The second second-order transition occurs when θ becomes equal to $\pi/2$ at the critical field H_c:

$$H_c = H_DH_a/H_e. \qquad (1.5.6.9)$$

After the reorientation transition, CoF_2 has the same magnetic point group as the weak ferromagnet NiF_2, *i.e.* $\boldsymbol{D}_{2h}(\boldsymbol{C}_{2h}) = mm'm'$.

1.5.7. Piezomagnetism

As we have seen, the appearance of weak ferromagnetism in antiferromagnets is closely connected with their magnetic symmetry. If the magnetic point group of the antiferromagnetic crystal contains an axis of higher than twofold symmetry, the magnetic structure is purely antiferromagnetic. By applying an external force that disturbs the symmetry of the crystal and destroys the axis of high symmetry, one may create a structure possessing weak ferromagnetism. In the previous section, we considered such reduction of the symmetry with the aid of a magnetic field applied perpendicular to the main axis of the crystal. Another possibility for symmetry reduction is to apply an external pressure and to deform the crystal. Thus, in some antiferromagnetic crystals, a ferromagnetic moment may be produced on application of external stress. This phenomenon is called piezomagnetism.

To investigate the piezomagnetic effect from the phenomenological point of view, we have to add the terms of the magnetoelastic energy in the expansion of the thermodynamic potential. The magnetoelastic terms of the least degree in the expansion of the thermodynamic potential $\tilde{\Phi}$ for a given stable magnetic structure will be of the type $T_{ij}M_kL_l$ (T_{ij} are the components of the elastic stress tensor **T**). These terms must be invariant relative

to the crystallographic group of the material under examination. If we consider the potential Φ, which is a function of T, $\mathbf{T}$, $\mathbf{H}$, the terms of the magnetoelastic energy that are responsible for piezomagnetism are of the form $H_i T_{jk}$. Thus, for the piezomagnetic crystals the expansion of the thermodynamic potential should be expressed by

$$\Phi(T, \mathbf{T}, \mathbf{H}) = \Phi_0(T, \mathbf{H}) - \Lambda_{ijk} H_i T_{jk}, \qquad (1.5.7.1)$$

where summation over the repeated indices i, j, k is implied. If at least one term of this expansion remains invariant under the magnetic symmetry of the given crystal, then the corresponding component Λ_{ijk} will not be zero and hence

$$\mu_0^* M_i = -\partial\Phi/\partial H_i = -\partial\Phi_0/\partial H_i + \Lambda_{ijk} T_{jk}. \qquad (1.5.7.2)$$

Thus, when a stress T_{jk} is applied, a magnetic moment is produced which is linear with the stress.

It follows from expression (1.5.7.1) that the converse of the piezomagnetic effect also exists, *i.e.* linear magnetostriction:

$$S_{jk} = -\partial\Phi/\partial T_{jk} = \Lambda_{ijk} H_i, \qquad (1.5.7.3)$$

where S_{jk} are the components of the deformation tensor.

1.5.7.1. *Piezomagnetic effect*

The possibility of the existence of a piezomagnetic effect was first foreseen by Voigt (1928). However, he assumed that it is sufficient to consider only the crystallographic symmetry in order to predict this effect. In reality, the crystals that do not possess a magnetic structure are characterized by the transformation R being contained in the magnetic group as an independent element. The transformation R changes the sign of the magnetic vectors **H**, **L**, **M**. Hence, for such crystals all values of Λ_{ijk} vanish and piezomagnetism is forbidden. The magnetic groups of magnetically ordered crystals (ferromagnets and antiferromagnets) contain R only in combination with other elements of symmetry, or do not contain this transformation at all. Hence the piezomagnetic effect may occur in such crystals. This statement was first made by Tavger & Zaitsev (1956). The most interesting manifestation of the piezomagnetic effect is observed in antiferromagnets, as there is no spontaneous magnetization in these materials.

From equation (1.5.7.1) it follows that Λ_{ijk} is an axial tensor of third rank. Hence, apart from the restriction that piezomagnetism is forbidden for all para- and diamagnetic materials, it must be absent from the 21 magnetic point groups that contain the element $C_i R = \bar{1}'$ (see Table 1.5.7.1). The stress tensor T_{jk} is symmetrical ($T_{jk} = T_{kj}$); see Section 1.3.2.4. Thus the tensor Λ_{ijk} is symmetrical in its last two indices. This is the reason why piezomagnetism is prohibited for three more magnetic point groups: $\boldsymbol{O} = 432$, $\boldsymbol{T}_d = \bar{4}3m$ and $\boldsymbol{O}_h = m\bar{3}m$. The remaining 66 magnetic point groups were found by Tavger (1958), who also constructed the 16 corresponding forms of the piezomagnetic tensors appropriate to each point group. They are represented in Table 1.5.7.1. (See also Birss & Anderson, 1963; Birss, 1964.)

Since the stress tensor T_{jk} is symmetrical, it has only six independent components. Therefore the notation of its components can be replaced by a matrix notation (Voigt's notation, see Section 1.3.2.5) in the following manner:

Tensor notation	Matrix notation
T_{11}	T_1
T_{22}	T_2
T_{33}	T_3
T_{23}, T_{32}	T_4
T_{31}, T_{13}	T_5
T_{12}, T_{21}	T_6

In matrix notation, equation (1.5.7.2) may be written in the form

$$\mu_0^* \delta M_i = -\partial(\Phi - \Phi_0)/\partial H_i = \Lambda_{ijk} T_{jk} = \Lambda_{i\alpha} T_\alpha, \qquad (1.5.7.4)$$

where $i = 1, 2, 3$ and $\alpha = 1, 2, 3, 4, 5, 6$. These notations are used in Table 1.5.7.1. Notice that $\Lambda_{ij} = \Lambda_{ijj}$ for $j = 1, 2, 3$, $\Lambda_{i4} = 2\Lambda_{i23}$, $\Lambda_{i5} = 2\Lambda_{i31}$, and $\Lambda_{i6} = 2\Lambda_{i12}$.

The form of the matrix $\Lambda_{i\alpha}$ depends on the orientation of the axes of the Cartesian coordinate system (CCS) with respect to the symmetry axes of the point group of the crystal under consideration. These symmetry axes may be rotation axes, rotoinversion axes or mirror-plane normals, all possibly combined with time reversal. The usual orientations of the CCS with respect to the symmetry axes can be expressed by the order of the entries in the Hermann–Mauguin symbol. An entry consists (apart from possible primes and bars) of a number $N = 1, 2, 3, 4$ or 6 or the letter m or N/m ($= \frac{N}{m}$). The conventional rules will be followed: in the monoclinic and orthorhombic crystal systems, the x, y and z axes of the CCS are parallel to the symmetry axes given in the first, second and third entries, respectively. In the monoclinic system, there is only one symmetry axis, which is usually chosen parallel to the y axis, and a short Hermann–Mauguin symbol with only one entry is usually used, *e.g.* $2/m$ instead of $1\,2/m\,1$. In the trigonal and hexagonal systems, the z, x and y axes are parallel to the symmetry axes given in the first, second and third entries, respectively. In the tetragonal system, the z axis is parallel to the symmetry axis given in the first entry, and the x and y axes are parallel to the symmetry axes given in the second entry, which appear in two mutually perpendicular directions. In the cubic system, the symmetry axes given in the first entry appear in three mutually perpendicular directions; the x, y and z axes of the CCS are chosen parallel to these directions. Alternative orientations of the same point group that give rise to the same form of $\Lambda_{i\alpha}$ have been added between square brackets [] in Table 1.5.7.1. Notice that the Schoenflies notation does not allow us to distinguish different orientations of the CCS with respect to the symmetry axes.

The forms of $\Lambda_{i\alpha}$ for frequently encountered orientations of the CCS other than those given in Table 1.5.7.1 are

(1) $112, 11m, 11\,2/m$ (unique axis z):

$$\begin{bmatrix} 0 & 0 & 0 & \Lambda_{14} & \Lambda_{15} & 0 \\ 0 & 0 & 0 & \Lambda_{24} & \Lambda_{25} & 0 \\ \Lambda_{31} & \Lambda_{32} & \Lambda_{33} & 0 & 0 & \Lambda_{36} \end{bmatrix};$$

(2) $112', 11m', 11\,2'/m'$ (unique axis z):

$$\begin{bmatrix} \Lambda_{11} & \Lambda_{12} & \Lambda_{13} & 0 & 0 & \Lambda_{16} \\ \Lambda_{21} & \Lambda_{22} & \Lambda_{23} & 0 & 0 & \Lambda_{26} \\ 0 & 0 & 0 & \Lambda_{34} & \Lambda_{35} & 0 \end{bmatrix};$$

(3) $211, m11, 2/m11$ (unique axis x):

$$\begin{bmatrix} \Lambda_{11} & \Lambda_{12} & \Lambda_{13} & \Lambda_{14} & 0 & 0 \\ 0 & 0 & 0 & 0 & \Lambda_{25} & \Lambda_{26} \\ 0 & 0 & 0 & 0 & \Lambda_{35} & \Lambda_{36} \end{bmatrix};$$

(4) $2'11, m'11, 2'/m'11$ (unique axis x):

$$\begin{bmatrix} 0 & 0 & 0 & 0 & \Lambda_{15} & \Lambda_{16} \\ \Lambda_{21} & \Lambda_{22} & \Lambda_{23} & \Lambda_{24} & 0 & 0 \\ \Lambda_{31} & \Lambda_{32} & \Lambda_{33} & \Lambda_{34} & 0 & 0 \end{bmatrix};$$

Table 1.5.7.1. *The forms of the matrix characterizing the piezomagnetic effect*

Magnetic crystal class		Matrix representation $\Lambda_{i\alpha}$ of the piezomagnetic tensor
Schoenflies	Hermann–Mauguin	
$\boldsymbol{C}_1$ $\boldsymbol{C}_i$	1 $\bar{1}$	$\begin{bmatrix} \Lambda_{11} & \Lambda_{12} & \Lambda_{13} & \Lambda_{14} & \Lambda_{15} & \Lambda_{16} \\ \Lambda_{21} & \Lambda_{22} & \Lambda_{23} & \Lambda_{24} & \Lambda_{25} & \Lambda_{26} \\ \Lambda_{31} & \Lambda_{32} & \Lambda_{33} & \Lambda_{34} & \Lambda_{35} & \Lambda_{36} \end{bmatrix}$
$\boldsymbol{C}_2$ $\boldsymbol{C}_s$ $\boldsymbol{C}_{2h}$	$2\,(=121)$ $m\,(=1m1)$ $2/m\,(=1\,2/m\,1)$ (unique axis y)	$\begin{bmatrix} 0 & 0 & 0 & \Lambda_{14} & 0 & \Lambda_{16} \\ \Lambda_{21} & \Lambda_{22} & \Lambda_{23} & 0 & \Lambda_{25} & 0 \\ 0 & 0 & 0 & \Lambda_{34} & 0 & \Lambda_{36} \end{bmatrix}$
$\boldsymbol{C}_2(\boldsymbol{C}_1)$ $\boldsymbol{C}_s(\boldsymbol{C}_1)$ $\boldsymbol{C}_{2h}(\boldsymbol{C}_i)$	$2'\,(=12'1)$ $m'\,(=1m'1)$ $2'/m'\,(=1\,2'/m'\,1)$ (unique axis y)	$\begin{bmatrix} \Lambda_{11} & \Lambda_{12} & \Lambda_{13} & 0 & \Lambda_{15} & 0 \\ 0 & 0 & 0 & \Lambda_{24} & 0 & \Lambda_{26} \\ \Lambda_{31} & \Lambda_{32} & \Lambda_{33} & 0 & \Lambda_{35} & 0 \end{bmatrix}$
$\boldsymbol{D}_2$ $\boldsymbol{C}_{2v}$ $\boldsymbol{D}_{2h}$	222 $mm2\,[2mm, m2m]$ mmm	$\begin{bmatrix} 0 & 0 & 0 & \Lambda_{14} & 0 & 0 \\ 0 & 0 & 0 & 0 & \Lambda_{25} & 0 \\ 0 & 0 & 0 & 0 & 0 & \Lambda_{36} \end{bmatrix}$
$\boldsymbol{D}_2(\boldsymbol{C}_2)$ $\boldsymbol{C}_{2v}(\boldsymbol{C}_2)$ $\boldsymbol{C}_{2v}(\boldsymbol{C}_s)$ $\boldsymbol{D}_{2h}(\boldsymbol{C}_{2h})$	$2'2'2$ $m'm'2$ $m'2'm\,[2'm'm]$ $m'm'm$	$\begin{bmatrix} 0 & 0 & 0 & 0 & \Lambda_{15} & 0 \\ 0 & 0 & 0 & \Lambda_{24} & 0 & 0 \\ \Lambda_{31} & \Lambda_{32} & \Lambda_{33} & 0 & 0 & 0 \end{bmatrix}$
$\boldsymbol{C}_4,\ \boldsymbol{C}_6$ $\boldsymbol{S}_4,\ \boldsymbol{C}_{3h}$ $\boldsymbol{C}_{4h},\ \boldsymbol{C}_{6h}$	$4,\ \underline{6}$ $\bar{4},\ \bar{6}$ $4/m,\ 6/m$	$\begin{bmatrix} 0 & 0 & 0 & \Lambda_{14} & \Lambda_{15} & 0 \\ 0 & 0 & 0 & \Lambda_{15} & -\Lambda_{14} & 0 \\ \Lambda_{31} & \Lambda_{31} & \Lambda_{33} & 0 & 0 & 0 \end{bmatrix}$
$\boldsymbol{C}_4(\boldsymbol{C}_2)$ $\boldsymbol{S}_4(\boldsymbol{C}_2)$ $\boldsymbol{C}_{4h}(\boldsymbol{C}_{2h})$	$4'$ $\bar{4}'$ $4'/m$	$\begin{bmatrix} 0 & 0 & 0 & \Lambda_{14} & \Lambda_{15} & 0 \\ 0 & 0 & 0 & -\Lambda_{15} & \Lambda_{14} & 0 \\ \Lambda_{31} & -\Lambda_{31} & 0 & 0 & 0 & \Lambda_{36} \end{bmatrix}$
$\boldsymbol{D}_4,\ \boldsymbol{D}_6$ $\boldsymbol{C}_{4v},\ \boldsymbol{C}_{6v}$ $\boldsymbol{D}_{2d},\ \boldsymbol{D}_{3h}$ $\boldsymbol{D}_{4h},\ \boldsymbol{D}_{6h}$	$422,\ 622$ $4mm,\ 6mm$ $\bar{4}2m\,[\bar{4}m2],\ \bar{6}m2\,[\bar{6}2m]$ $4/mmm,\ 6/mmm$	$\begin{bmatrix} 0 & 0 & 0 & \Lambda_{14} & 0 & 0 \\ 0 & 0 & 0 & 0 & -\Lambda_{14} & 0 \\ 0 & 0 & 0 & 0 & 0 & 0 \end{bmatrix}$
$\boldsymbol{D}_4(\boldsymbol{C}_4),\ \boldsymbol{D}_6(\boldsymbol{C}_6)$ $\boldsymbol{C}_{4v}(\boldsymbol{C}_4),\ \boldsymbol{C}_{6v}(\boldsymbol{C}_6)$ $\boldsymbol{D}_{2d}(\boldsymbol{S}_4),\ \boldsymbol{D}_{3h}(\boldsymbol{C}_{3h})$ $\boldsymbol{D}_{4h}(\boldsymbol{C}_{4h}),\ \boldsymbol{D}_{6h}(\boldsymbol{C}_{6h})$	$42'2',\ 62'2'$ $4m'm',\ 6m'm'$ $\bar{4}2'm'\,[\bar{4}m'2'],\ \bar{6}m'2'\,[\bar{6}2'm']$ $4/mm'm',\ 6/mm'm'$	$\begin{bmatrix} 0 & 0 & 0 & 0 & \Lambda_{15} & 0 \\ 0 & 0 & 0 & \Lambda_{15} & 0 & 0 \\ \Lambda_{31} & \Lambda_{31} & \Lambda_{33} & 0 & 0 & 0 \end{bmatrix}$
$\boldsymbol{D}_4(\boldsymbol{D}_2)$ $\boldsymbol{C}_{4v}(\boldsymbol{C}_{2v})$ $\boldsymbol{D}_{2d}(\boldsymbol{D}_2),\ \boldsymbol{D}_{2d}(\boldsymbol{C}_{2v})$ $\boldsymbol{D}_{4h}(\boldsymbol{D}_{2h})$	$4'22'$ $4'mm'$ $\bar{4}'2m',\ \bar{4}'m2'$ $4'/mmm'$	$\begin{bmatrix} 0 & 0 & 0 & \Lambda_{14} & 0 & 0 \\ 0 & 0 & 0 & 0 & \Lambda_{14} & 0 \\ 0 & 0 & 0 & 0 & 0 & \Lambda_{36} \end{bmatrix}$
$\boldsymbol{C}_3$ $\boldsymbol{S}_6$	$\underline{3}$ $\bar{3}$	$\begin{bmatrix} \Lambda_{11} & -\Lambda_{11} & 0 & \Lambda_{14} & \Lambda_{15} & -2\Lambda_{22} \\ -\Lambda_{22} & \Lambda_{22} & 0 & \Lambda_{15} & -\Lambda_{14} & -2\Lambda_{11} \\ \Lambda_{31} & \Lambda_{31} & \Lambda_{33} & 0 & 0 & 0 \end{bmatrix}$
$\boldsymbol{D}_3$ $\boldsymbol{C}_{3v}$ $\boldsymbol{D}_{3d}$	$32\,(=321)$ $\underline{3}m\,(=\underline{3}m1)$ $\bar{3}m\,(=\bar{3}m1)$	$\begin{bmatrix} \Lambda_{11} & -\Lambda_{11} & 0 & \Lambda_{14} & 0 & 0 \\ 0 & 0 & 0 & 0 & -\Lambda_{14} & -2\Lambda_{11} \\ 0 & 0 & 0 & 0 & 0 & 0 \end{bmatrix}$
$\boldsymbol{D}_3(\boldsymbol{C}_3)$ $\boldsymbol{C}_{3v}(\boldsymbol{C}_3)$ $\boldsymbol{D}_{3d}(\boldsymbol{S}_6)$	$32'\,(=32'1)$ $\underline{3}m'\,(=\underline{3}m'1)$ $\bar{3}m'\,(=\bar{3}m'1)$	$\begin{bmatrix} 0 & 0 & 0 & 0 & \Lambda_{15} & -2\Lambda_{22} \\ -\Lambda_{22} & \Lambda_{22} & 0 & \Lambda_{15} & 0 & 0 \\ \Lambda_{31} & \Lambda_{31} & \Lambda_{33} & 0 & 0 & 0 \end{bmatrix}$
$\boldsymbol{C}_6(\boldsymbol{C}_3)$ $\boldsymbol{C}_{3h}(\boldsymbol{C}_3)$ $\boldsymbol{C}_{6h}(\boldsymbol{S}_6)$	$\underline{6}'$ $\bar{6}'$ $6'/m'$	$\begin{bmatrix} \Lambda_{11} & -\Lambda_{11} & 0 & 0 & 0 & -2\Lambda_{22} \\ -\Lambda_{22} & \Lambda_{22} & 0 & 0 & 0 & -2\Lambda_{11} \\ 0 & 0 & 0 & 0 & 0 & 0 \end{bmatrix}$
$\boldsymbol{D}_6(\boldsymbol{D}_3)$ $\boldsymbol{C}_{6v}(\boldsymbol{C}_{3v})$ $\boldsymbol{D}_{3h}(\boldsymbol{D}_3),\ \boldsymbol{D}_{3h}(\boldsymbol{C}_{3v})$ $\boldsymbol{D}_{6h}(\boldsymbol{D}_{3d})$	$6'22'$ $6'mm'$ $\bar{6}'2m',\ \bar{6}'m2'$ $6'/m'mm'$	$\begin{bmatrix} \Lambda_{11} & -\Lambda_{11} & 0 & 0 & 0 & 0 \\ 0 & 0 & 0 & 0 & 0 & -2\Lambda_{11} \\ 0 & 0 & 0 & 0 & 0 & 0 \end{bmatrix}$
$\boldsymbol{T},\ \boldsymbol{T}_h$ $\boldsymbol{O}(\boldsymbol{T})$ $\boldsymbol{T}_d(\boldsymbol{T})$ $\boldsymbol{O}_h(\boldsymbol{T}_h)$	$23,\ m\bar{3}$ $4'32'$ $\bar{4}'3m'$ $m\bar{3}m'$	$\begin{bmatrix} 0 & 0 & 0 & \Lambda_{14} & 0 & 0 \\ 0 & 0 & 0 & 0 & \Lambda_{14} & 0 \\ 0 & 0 & 0 & 0 & 0 & \Lambda_{14} \end{bmatrix}$

(5) $22'2'$, $2m'm'$, $mm'2'$ $[m2'm']$, $mm'm'$:

$$\begin{bmatrix} \Lambda_{11} & \Lambda_{12} & \Lambda_{13} & 0 & 0 & 0 \\ 0 & 0 & 0 & 0 & 0 & \Lambda_{26} \\ 0 & 0 & 0 & 0 & \Lambda_{35} & 0 \end{bmatrix};$$

(6) $2'22'$, $m'2m'$, $2'mm'$ $[m'm2']$, $m'mm'$:

$$\begin{bmatrix} 0 & 0 & 0 & 0 & 0 & \Lambda_{16} \\ \Lambda_{21} & \Lambda_{22} & \Lambda_{23} & 0 & 0 & 0 \\ 0 & 0 & 0 & \Lambda_{34} & 0 & 0 \end{bmatrix};$$

(7) $4'2'2$, $4'm'm$, $\overline{4}'m'2$, $\overline{4}'2'm$, $4'/mm'm$:

$$\begin{bmatrix} 0 & 0 & 0 & 0 & \Lambda_{15} & 0 \\ 0 & 0 & 0 & -\Lambda_{15} & 0 & 0 \\ \Lambda_{31} & -\Lambda_{31} & 0 & 0 & 0 & 0 \end{bmatrix};$$

(8) $6'2'2$, $6'm'm$, $\overline{6}'m'2$, $\overline{6}'2'm$, $6'/m'm'm$:

$$\begin{bmatrix} 0 & 0 & 0 & 0 & 0 & -2\Lambda_{22} \\ -\Lambda_{22} & \Lambda_{22} & 0 & 0 & 0 & 0 \\ 0 & 0 & 0 & 0 & 0 & 0 \end{bmatrix};$$

(9) 312, $31m$, $\overline{3}1m$:

$$\begin{bmatrix} 0 & 0 & 0 & \Lambda_{14} & 0 & -2\Lambda_{22} \\ -\Lambda_{22} & \Lambda_{22} & 0 & 0 & -\Lambda_{14} & 0 \\ 0 & 0 & 0 & 0 & 0 & 0 \end{bmatrix};$$

(10) $312'$, $31m'$, $\overline{3}1m'$:

$$\begin{bmatrix} \Lambda_{11} & -\Lambda_{11} & 0 & 0 & \Lambda_{15} & 0 \\ 0 & 0 & 0 & \Lambda_{15} & 0 & -2\Lambda_{11} \\ \Lambda_{31} & \Lambda_{31} & \Lambda_{33} & 0 & 0 & 0 \end{bmatrix}.$$

Many connections between the different forms of $\Lambda_{i\alpha}$ given above and in Table 1.5.7.1 have been derived by Kopský (1979*a*,*b*) and Grimmer (1991). These connections between the forms that the matrix can assume for the various magnetic or crystallographic point groups hold for all matrices and tensors that describe properties of materials, not just for the special case of piezomagnetism.

Dzyaloshinskii (1957*b*) pointed out a number of antiferromagnets that may display the piezomagnetic effect. These include the fluorides of the transition metals, in which the piezomagnetic effect was first observed experimentally (see Fig. 1.5.7.1) (Borovik-Romanov, 1959*b*). Below we shall discuss the origin of the piezomagnetic effect in fluorides in more detail.

The fluorides of transition metals MnF_2, CoF_2 and FeF_2 are tetragonal easy-axis antiferromagnets (see Fig. 1.5.5.3). It is easy to check that the expansion of the thermodynamic potential $\tilde{\Phi}$ up to terms that are linear in stress T_{ij} and invariant relative to the transformations of the crystallographic space group $\boldsymbol{D}_{4h}^{14} = P4_2/mnm$ is represented by

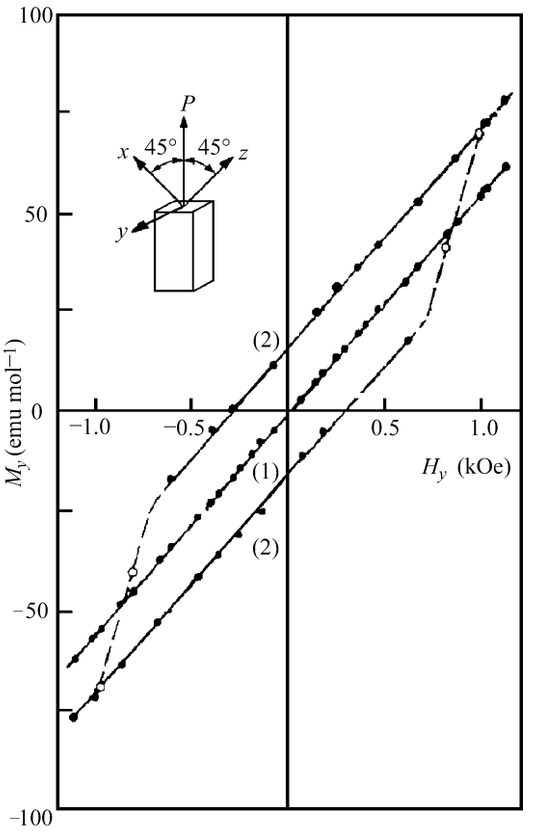

Fig. 1.5.7.1. The dependence of the magnetic moment of CoF_2 on the magnetic field. (1) Without stress; (2) under the stress T_{xz} = 33.3 MPa (Borovik-Romanov, 1960). (H = 1 kOe corresponds to B = 1 kG = 0.1 T; M = 100 emu mol^{-1} = 0.1 A m^2 mol^{-1}.)

$$\begin{aligned} \tilde{\Phi} = \tilde{\Phi}_0 &+ (A/2)\mathbf{L}^2 + (a/2)(L_x^2 + L_y^2) \\ &+ (B/2)\mathbf{M}^2 + (b/2)(M_x^2 + M_y^2) \\ &+ d(L_x M_y + L_y M_x) \\ &+ 2\lambda_1(M_x T_{yz} + M_y T_{xz})L_z \\ &+ 2\eta_1(L_y T_{yz} + L_x T_{xz})L_z \\ &+ 2\lambda_2 M_z L_z T_{xy} + 2\eta_2 L_x L_y T_{xy} - \mu_0^* \mathbf{MH}. \end{aligned} \tag{1.5.7.5}$$

In this expression, the sums $(T_{ij} + T_{ji})$ that appear in the magnetoelastic terms have been replaced by $2T_{ij}$, as $T_{ij} \equiv T_{ji}$.

The analysis of expression (1.5.7.5) in the absence of stresses proves that fluorides may possess weak ferromagnetism provided that $a < 0$ ($L_z = 0$) (see Section 1.5.5.1). Here we shall discuss the easy-axis structure of the fluorides MnF_2, CoF_2, FeF_2 (see Fig. 1.5.5.3*b*). In the absence of magnetic fields and stresses only $L_z \neq 0$ for this structure. All other components of the vector $\mathbf{L}$ and the magnetization vector $\mathbf{M}$ are equal to zero. The magnetic point group is $\boldsymbol{D}_{4h}(\boldsymbol{D}_{2h}) = 4'/mmm'$.

To transform the potential $\tilde{\Phi}(L_i, M_j, T_{k\ell})$ [(1.5.7.5)] into the form $\Phi(T, \mathbf{T}, \mathbf{H})$ [(1.5.7.1)], one has to insert into the magnetoelastic terms the dependence of the components of $\mathbf{L}$ and $\mathbf{M}$ on the magnetic field. The corresponding relations, obtained by minimization of (1.5.7.5) without the magnetoelastic terms, are

$$\begin{aligned} M_x &= \frac{\mu_0^* a}{a(B+b) - d^2} H_x; \quad & L_x &= -\frac{\mu_0^* d}{a(B+b) - d^2} H_y; \\ M_y &= \frac{\mu_0^* a}{a(B+b) - d^2} H_y; \quad & L_y &= -\frac{\mu_0^* d}{a(B+b) - d^2} H_x; \\ M_z &= \frac{\mu_0^*}{B} H_z; & L_z &\simeq \text{constant}. \end{aligned} \tag{1.5.7.6}$$

To a first approximation, the component L_z does not depend on the magnetic field.

Inserting the relations (1.5.7.6) for M_i and L_i into the magnetoelastic terms of (1.5.7.5), one gets the following expression for the corresponding terms in $\Phi(T, H_i, T_{jk})$:

$$\Phi(T, H_i, T_{jk}) = \Phi_0(T, H_i) + \mu_0^* \Big[2L_z \frac{a\lambda_1 - d\eta_1}{a(B+b) - d^2} T_{yz} H_x + 2L_z \frac{a\lambda_1 - d\eta_1}{a(B+b) - d^2} T_{xz} H_y + 2L_z \frac{\lambda_2}{B} T_{xy} H_z \Big]. \quad (1.5.7.7)$$

In this case, the expression for the magnetoelastic energy contains only three components of the stress tensor: T_{yz}, T_{xz} and T_{xy}. Using (1.5.7.4), we get formulas for the three main components of the piezomagnetic effect:

$$\delta M_x = 2L_z \frac{d\eta_1 - a\lambda_1}{a(B+b) - d^2} T_{yz} = 2\Lambda_{xyz} T_{yz} = \Lambda_{14} T_4, \quad (1.5.7.8)$$

$$\delta M_y = 2L_z \frac{d\eta_1 - a\lambda_1}{a(B+b) - d^2} T_{xz} = 2\Lambda_{yxz} T_{xz} = \Lambda_{25} T_5, \quad (1.5.7.9)$$

$$\delta M_z = -2L_z \frac{\lambda_2}{B} T_{xy} = 2\Lambda_{zxy} T_{xy} = \Lambda_{36} T_6. \quad (1.5.7.10)$$

In all three cases, the piezomagnetic moment is produced in the direction perpendicular to the shear plane. Comparing (1.5.7.8) and (1.5.7.9), we see that $\Lambda_{25} = \Lambda_{14}$. This is in agreement with the equivalence of the axes x and y in the tetragonal crystals. If the stress is applied in the plane xz (or yz), the vector **L** turns in the shear plane and a component L_x (or L_y) is produced:

$$L_x = 2L_z \frac{\eta_1(B+b) - d\lambda_1}{a(B+b) - d^2} T_{xz}. \quad (1.5.7.11)$$

For T_{xy} stress, no rotation of the vector **L** occurs.

Formulas (1.5.7.8)–(1.5.7.10) show that in accordance with Table 1.5.7.1 the form of the matrix $\Lambda_{i\alpha}$ for the magnetic point group $\boldsymbol{D}_{4h}(\boldsymbol{D}_{2h}) = 4'/mmm'$ is

$$\boldsymbol{\Lambda}_{i\alpha} = \begin{bmatrix} 0 & 0 & 0 & \Lambda_{14} & 0 & 0 \\ 0 & 0 & 0 & 0 & \Lambda_{14} & 0 \\ 0 & 0 & 0 & 0 & 0 & \Lambda_{36} \end{bmatrix}. \quad (1.5.7.12)$$

The relations (1.5.7.8)–(1.5.7.10) show that the components of the piezomagnetic tensor Λ_{ijk} are proportional to the components of the antiferromagnetic vector **L**. Thus the sign of the piezomagnetic moment depends on the sign of the vector **L** and the value of the piezomagnetic effect depends on the domain structure of the sample (we are referring to S-domains). The piezomagnetic moment may become equal to zero in a polydomain sample. On the other hand, piezomagnetism may be used to obtain single-domain antiferromagnetic samples by cooling them from the paramagnetic state in a magnetic field under suitably oriented external pressure.

There are relatively few publications devoted to experimental investigations of the piezomagnetic effect. As mentioned above, the first measurements of the values of the components of the tensor Λ_{ijk} were performed on crystals of MnF_2 and CoF_2 (Borovik-Romanov, 1960). In agreement with theoretical prediction, three components were observed: $\Lambda_{xyz} = \Lambda_{yxz}$ and Λ_{zxy}. The largest value obtained for these components was $\Lambda_{14} = 21 \times 10^{-10}$ Oe^{-1} $= 26 \times 10^{-12}$ m A^{-1}. The piezomagnetic effect was also observed for two modifications of α-Fe_2O_3 (Andratskii & Borovik-Romanov, 1966). The magnetic point group of the low-temperature modification of this compound is $\boldsymbol{D}_{3d} = \bar{3}m$. In accordance with form (7) given above, the following nonzero components Λ_{ijk} were found for the low-temperature state:

$$\Lambda_{xyz} = -\Lambda_{yxz}, \quad (1.5.7.13)$$

$$\Lambda_{yyy} = -\Lambda_{yxx} = -\Lambda_{xxy}. \quad (1.5.7.14)$$

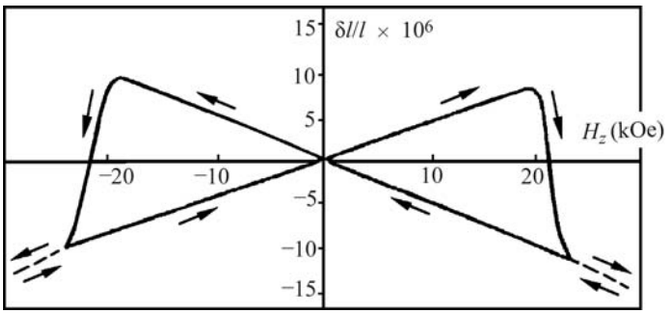

Fig. 1.5.7.2. Linear magnetostriction of CoF_2 (Prokhorov & Rudashevskii, 1975). (H = 1 kOe corresponds to B = 1 kG = 0.1 T.)

The values of these components are one order of magnitude smaller than for CoF_2.

The temperature dependence of the components is similar for the piezomagnetic tensor and the sublattice magnetization. This means that the magnetoelastic constants λ_1 and λ_2 (as well as the constants B and d) in the relations (1.5.7.7) and (1.5.7.8) depend only slightly on temperature.

1.5.7.2. *Linear magnetostriction*

From expression (1.5.7.3), it follows that a deformation of the sample may occur in a magnetic field. This deformation is linear with respect to the field. By its linear dependence, this effect differs essentially from ordinary magnetostriction, which is quadratic in the magnetic field. Most substances display such quadratic magnetostriction. The linear magnetostriction may be observed only in those crystals that belong to one of the 66 magnetic point groups that allow piezomagnetism. They are listed in Table 1.5.7.1. The distinctive feature of linear magnetostriction is the dependence of its sign on the sign of the magnetic field and on the sign of the antiferromagnetic vector **L**. The sign of **L** characterizes the domain state of the specimen. Thus, observation of linear magnetostriction gives information about the domain state. In some materials, it has been observed that a sudden transition from one domain state to the opposite may occur in strong magnetic fields.

Linear magnetostriction (LM) was observed in CoF_2 by Borovik-Romanov & Yavelov (1963) in a magnetic field applied parallel to the fourfold axis. The relations for the LM in CoF_2 can be obtained by differentiating the expression of the thermodynamic potential Φ [(1.5.7.7)]. If the magnetic field is applied along the y axis, a deformation S_{xz} appears:

$$S_{xz} = -\partial\Phi/\partial T_{xz} = 2\mu_0^* L_z \frac{d\eta_1 - a\lambda_1}{a(B+b) - d^2} H_y = 2\Lambda_{yxz} H_y = \Lambda_{25} H_2. \quad (1.5.7.15)$$

A similar formula holds for S_{yz} if the magnetic field is applied parallel to the x axis (with Λ_{14}, which is equal to Λ_{25}).

If the magnetic field is applied parallel to the fourfold axis, the S_{xy} component of the deformation appears:

$$S_{xy} = -\partial\Phi/\partial T_{xy} = -2\mu_0^* L_z(\lambda_2/B) H_z = -2\mu_0^* L_z \lambda_2 \chi_\parallel H_z = 2\Lambda_{zxy} H_z = \Lambda_{36} H_3. \quad (1.5.7.16)$$

If the relations (1.5.7.15) and (1.5.7.16) are compared with (1.5.7.8)–(1.5.7.10), it is apparent that in accordance with theory the components of the tensors of the piezomagnetic effect (PM) and LM are identical.

Prokhorov & Rudashevskii (1969, 1975) extended the investigation of LM in CoF_2. They discovered that if the applied field becomes larger than 20 kOe (B_z > 20 kG = 2 T), a jump in the magnetostriction occurs and it changes its sign (see Fig. 1.5.7.2). This jump is the result of a transition of the magnetic structure

Table 1.5.7.2. *Experimental data for the piezomagnetic effect (PM) and for linear magnetostriction (LM)*

a: antiferromagnetic phase; *w*: weak ferromagnetic phase.

Compound	$\Lambda_{i\alpha} \times 10^{10}$ (Oe^{-1})	T (K)	PM or LM	Reference†
MnF_2	$\Lambda_{14} \simeq 0.2$	20	PM	(1)
CoF_2	$\Lambda_{14} = 21$	20	PM	(1)
	$\Lambda_{36} = 8.2$	20	PM	(1)
	$\Lambda_{36} = 9.8$	4	LM	(3)
$DyFeO_3$	$\Lambda_{36} = 6.0$	6	LM	(8)
$YFeO_3$	$\Lambda_{15} = 1.7$	6	LM	(6)
$YCrO_3$	$\Lambda_{15} \simeq 1$	6	LM	(7)
α-Fe_2O_3 (*a*)	$\Lambda_{22} = 1.9$	78	LM	(4)
	$\Lambda_{22} = 3.2$	77	PM	(2)
	$\Lambda_{22} = 1.3$	100	LM	(5)
	$\Lambda_{14} = 0.3$	78	LM	(4)
	$\Lambda_{14} = 1.7$	77	PM	(2)
	$\Lambda_{14} = 0.9$	100	LM	(5)
α-Fe_2O_3 (*w*)	$\Lambda_{23} = 2.5$	292	PM	(2)

† References: (1) Borovik-Romanov (1959*b*, 1960); (2) Andratskii & Borovik-Romanov (1966); (3) Prokhorov & Rudashevskii (1969, 1975); (4) Anderson *et al.* (1964); (5) Levitin & Shchurov (1973); (6) Kadomtseva, Agafonov, Milov *et al.* (1981); (7) Kadomtseva, Agafonov, Lukina *et al.* (1981); (8) Zvezdin *et al.* (1985).

from one domain state ($\mathbf{L}_+$) into the opposite state ($\mathbf{L}_-$). To explain such a transition, one has to take into account the term of third power in the expansion of the magnetic energy (Scott & Anderson, 1966),

$$U_m = A_i H_i + \tfrac{1}{2}\chi_{ij} H_i H_j + C_{ijk} H_i H_j H_k. \qquad (1.5.7.17)$$

C_{ijk} is an axial time-antisymmetric tensor, the sign of which depends on the sign of the domain. This term defines the dependence of the magnetic energy on the sign of the antiferromagnetic domain.

To date, CoF_2 and MnF_2 are unique in that LM and PM occur without rotating the antiferromagnetic vector $\mathbf{L}$ if the magnetic field is applied along the fourfold axis (or pressure along a ⟨110⟩ axis). In all other cases, these effects are accompanied by a rotation of $\mathbf{L}$ and, as a result, the creation of new components L_i. To the latter belongs the LM in the low-temperature modification of α-Fe_2O_3, which was observed by Anderson *et al.* (1964) (see also Scott & Anderson, 1966; Levitin & Shchurov, 1973). This compound displays PM, therefore it is obvious that LM will also occur (see Table 1.5.7.1).

LM has been observed in some orthoferrites. At low temperatures, the orthoferrite $DyFeO_3$ is a pure antiferromagnet, the vector $\mathbf{L}$ of which is aligned along the y axis. Its magnetic point group ($\boldsymbol{D}_{2h} = mmm$) allows PM and LM. The latter was observed when a magnetic field was applied parallel to the z axis by Zvezdin *et al.* (1985). There it was shown that $\Lambda_{zxy} \neq 0$ if $0 < H < H_c$. At $H_c \simeq 4$ kOe ($B_c \simeq 4$ kG = 0.4 T), there occurs a first-order phase transition into a weakly ferromagnetic state with magnetic point group $\boldsymbol{D}_{2h}(\boldsymbol{C}_{2h}) = m'm'm$ ($\mathbf{L} \parallel Ox, \mathbf{M}_D \parallel Oz$).

Many orthoferrites and orthochromites that possess weak ferromagnetism belong to the same point group, which possesses an ordinary centre of symmetry. Thus PM and LM are allowed for these phases of orthoferrites. If the magnetic field is applied parallel to Ox, they undergo a reorientation transition at which both vectors, $\mathbf{L}$ and $\mathbf{M}_D$, being orthogonal, rotate in the xz plane. These intermediate angular phases belong to the magnetic point group $\boldsymbol{C}_{2h}(\boldsymbol{C}_i) = 2'/m'$.

LM was observed by Kadomtseva and coworkers (Kadomtseva, Agafonov, Lukina *et al.*, 1981; Kadomtseva, Agafonov, Milov *et al.*, 1981) in two such compounds, $YFeO_3$ and $YCrO_3$. They measured the Λ_{xxz} components of the LM tensor, which are allowed for the $\boldsymbol{D}_{2h}(\boldsymbol{C}_{2h}) = m'm'm$ state.

The experimental data obtained to date for PM and LM are summarized in Table 1.5.7.2. The values of the components $\Lambda_{i\alpha}$ can be converted to SI units using 1 Oe^{-1} = $4\pi \times 10^{-3}$ m A^{-1} = $4\pi \times 10^{-3}$ T Pa^{-1}.

1.5.7.3. *Linear magnetic birefringence*

The magnetic contribution to the component of the relative permittivity $\delta\varepsilon_{ij}$ can be represented as a series in the powers of the components of the magnetization and the antiferromagnetic vector. The magnetic birefringence (also called the Cotton–Mouton or Voigt effect) is described by the real symmetrical part of the tensor $\delta\varepsilon_{ij}$. In paramagnetic crystals, the magnetization $\mathbf{M}$ is proportional to the applied magnetic field $\mathbf{H}$, and the series has the form

$$\delta\varepsilon_{ij} = Q^{MM}_{ijk\ell} M_k M_\ell = Q^{MM}_{ijk\ell} \chi^M_{kr} \chi^M_{\ell s} H_r H_s = \Gamma_{ijrs} H_r H_s. \qquad (1.5.7.18)$$

The tensor Γ_{ijrs} is symmetric with respect to both the first and the second pair of indices. The symmetry of this tensor implies that the diagonal components of the permittivity tensor include magnetic corrections. The modification of the diagonal components gives rise to birefringence in cubic crystals and to a change $\Delta n^{\rm pm}$ of the birefringence in uniaxial and lower-symmetry crystals. It follows from (1.5.7.18) that this birefringence is bilinear in the applied field. Bilinear magnetic birefringence can be observed in uniaxial crystals if the magnetic field is applied along the x axis perpendicular to the principal z axis. In the simplest case, a difference in the refractive indices n_x and n_y arises:

$$\Delta n^{\rm pm} = n_x - n_y = \frac{1}{2n_0}(\delta\varepsilon_{xx} - \delta\varepsilon_{yy}) = \frac{1}{2n_0}(\Gamma_{xxxx} - \Gamma_{yyxx}) H_x^2, \qquad (1.5.7.19)$$

where n_0 is the refractive index for the ordinary beam.

Consider now a magnetically ordered crystal which can be characterized by an antiferromagnetic vector $\mathbf{L}_0$ and a magnetization vector $\mathbf{M}_0$ in the absence of a magnetic field. Applying a magnetic field with components H_r, we change the direction and size of $\mathbf{L}_0$ and $\mathbf{M}_0$, getting additional components $L^H_k = \chi^L_{kr} H_r$ and $M^H_k = \chi^M_{kr} H_r$. This is illustrated by the relations (1.5.7.6). Instead of (1.5.7.18) we get

$$\begin{aligned}\delta\varepsilon_{ij} &= Q^{LL}_{ijk\ell} L_k L_\ell + Q^{ML}_{ijk\ell} M_k L_\ell + Q^{MM}_{ijk\ell} M_k M_\ell \\ &= Q^{LL}_{ijk\ell} L_{0k} L_{0\ell} + Q^{ML}_{ijk\ell} M_{0k} L_{0\ell} + Q^{MM}_{ijk\ell} M_{0k} M_{0\ell} \\ &\quad + [2Q^{LL}_{ijk\ell} \chi^L_{kr} L_{0\ell} + Q^{ML}_{ijk\ell}(\chi^M_{kr} L_{0\ell} + M_{0k} \chi^L_{\ell r}) + 2Q^{MM}_{ijk\ell} \chi^M_{kr} M_{0\ell}] H_r. \end{aligned} \qquad (1.5.7.20)$$

The terms in the middle line of (1.5.7.20) show that, in an ordered state, a change in the refractive indices occurs that is proportional to L_0^2 in antiferromagnets and to M_0^2 in ferromagnets. The terms in square brackets show that a linear magnetic birefringence may exist. In the special case of a tetragonal antiferromagnet belonging to the space group $\boldsymbol{D}^{14}_{4h} = P4_2/mnm$ with $\mathbf{L}_0$ parallel to the principal axis z, the linear birefringence occurs in the xy plane if the magnetic field is applied along the z axis (see Fig. 1.5.5.3). In this case, $\mathbf{M}_0 = 0$, $\chi^L_{kz} = 0$ for all k, $\chi^M_{xz} = \chi^M_{yz} = 0$ and $\chi^M_{zz} = \mu_0^*/B$ [see (1.5.7.6)]. Therefore, the terms in square brackets in (1.5.7.20) differ from zero only for one component of $\delta\varepsilon_{ij}$,

$$\delta\varepsilon_{xy} = Q^{ML}_{xyzz} L_{0z} \mu_0^* H_z / B = q_{zxy} \mu_0^* H_z \,\mathrm{sign}(L_{0z}). \qquad (1.5.7.21)$$

As a result,

$$\Delta n^{\rm af} = n_{x'} - n_{y'} = \frac{1}{2n_0}\delta\varepsilon_{xy} = \frac{1}{2n_0} q_{zxy} \mu_0^* H_z \,\mathrm{sign}(L_{0z}), \qquad (1.5.7.22)$$

where x', y' are the optic axes, which in these tetragonal crystals are rotated by $\pi/4$ relative to the crystallographic axes.

Comparing relation (1.5.7.22) with (1.5.7.3), one can see that, like LM, there may be linear magnetic birefringence. The forms of the tensors that describe the two effects are the same.

Linear magnetic birefringence has been observed in the uniaxial antiferromagnetic low-temperature modification of α-Fe_2O_3

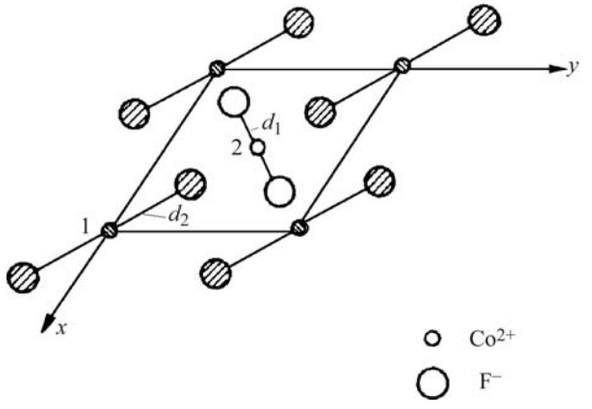

Fig. 1.5.7.3. Variation of symmetry of the crystal field in the presence of the piezomagnetic effect in CoF_2. The unshaded atoms lie at height $c/2$ above the xy plane (see Fig. 1.5.5.3).

when the magnetic field was applied perpendicular to the threefold axis (Le Gall *et al.*, 1977; Merkulov *et al.*, 1981). The most impressive effect was observed in CoF_2 when the magnetic field was applied along the fourfold axis. The crystal ceased to be optically uniaxial and a difference $(n_{x'} - n_{y'}) \propto H_z$ was observed, in accordance with (1.5.7.22). Such linear magnetic birefringence does not exist in the paramagnetic state. Linear birefringence has been observed also in $CoCO_3$ and $DyFeO_3$. For details of these experiments, see Eremenko *et al.* (1989). These authors also used linear birefringence to make the antiferromagnetic domains visible. A further review of linear magnetic birefringence has been given by Ferré & Gehring (1984).

Piezomagnetism, linear magnetostriction and linear birefringence in fluorides can be clearly demonstrated qualitatively for one particular geometry. As shown in Fig. 1.5.7.3, the crystallographically equivalent points 1 and 2 are no longer equivalent after a shear deformation applied in the plane xy. During such a deformation, the distances from the magnetic ions to the nearest fluoride ions increase in points 1 and decrease in points 2. As a result, the values of the g-factors for the ions change. Evidently, the changes of the values of the g-factors for different sublattices are opposite in sign. Thus the sublattice magnetizations are no longer equal, and a magnetic moment arises along the direction of sublattice magnetization. On the other hand, if we increase the magnetization of one sublattice and decrease the magnetization of the other by applying a magnetic field parallel to the z axis, the interactions with the neighbouring fluoride ions also undergo changes with opposite signs. This gives rise to the magnetostriction. These considerations can be applied only to antiferromagnets with the fluoride structure. In these structures, single-ion anisotropy is responsible for the weak ferromagnetism, not the antisymmetric exchange interaction of the form $\mathbf{d}[\mathbf{S}_i \times \mathbf{S}_k]$.

Table 1.5.8.1. *The forms of the tensor characterizing the linear magnetoelectric effect*

Magnetic crystal class		Matrix representation of the property tensor α_{ij}
Schoenflies	Hermann–Mauguin	
$\boldsymbol{C}_1$ $\boldsymbol{C}_i(\boldsymbol{C}_1)$	1 $\bar{1}'$	$\begin{bmatrix} \alpha_{11} & \alpha_{12} & \alpha_{13} \\ \alpha_{21} & \alpha_{22} & \alpha_{23} \\ \alpha_{31} & \alpha_{32} & \alpha_{33} \end{bmatrix}$
$\boldsymbol{C}_2$ $\boldsymbol{C}_s(\boldsymbol{C}_1)$ $\boldsymbol{C}_{2h}(\boldsymbol{C}_2)$	$2\,(=121)$ $m'\,(=1m'1)$ $2/m'\,(=1\,2/m'\,1)$ (unique axis y)	$\begin{bmatrix} \alpha_{11} & 0 & \alpha_{13} \\ 0 & \alpha_{22} & 0 \\ \alpha_{31} & 0 & \alpha_{33} \end{bmatrix}$
$\boldsymbol{C}_s$ $\boldsymbol{C}_2(\boldsymbol{C}_1)$ $\boldsymbol{C}_{2h}(\boldsymbol{C}_s)$	$m\,(=1m1)$ $2'\,(=12'1)$ $2'/m\,(=1\,2'/m\,1)$ (unique axis y)	$\begin{bmatrix} 0 & \alpha_{12} & 0 \\ \alpha_{21} & 0 & \alpha_{23} \\ 0 & \alpha_{32} & 0 \end{bmatrix}$
$\boldsymbol{D}_2$ $\boldsymbol{C}_{2v}(\boldsymbol{C}_2)$ $\boldsymbol{D}_{2h}(\boldsymbol{D}_2)$	222 $m'm'2\,[2m'm',\ m'2m']$ $m'm'm'$	$\begin{bmatrix} \alpha_{11} & 0 & 0 \\ 0 & \alpha_{22} & 0 \\ 0 & 0 & \alpha_{33} \end{bmatrix}$
$\boldsymbol{C}_{2v}$ $\boldsymbol{D}_2(\boldsymbol{C}_2)$ $\boldsymbol{C}_{2v}(\boldsymbol{C}_s)$ $\boldsymbol{D}_{2h}(\boldsymbol{C}_{2v})$	$mm2$ $2'2'2$ $2'mm'\,[m2'm']$ mmm'	$\begin{bmatrix} 0 & \alpha_{12} & 0 \\ \alpha_{21} & 0 & 0 \\ 0 & 0 & 0 \end{bmatrix}$
$\boldsymbol{C}_4,\ \boldsymbol{S}_4(\boldsymbol{C}_2),\ \boldsymbol{C}_{4h}(\boldsymbol{C}_4)$ $\boldsymbol{C}_3,\ \boldsymbol{S}_6(\boldsymbol{C}_3)$ $\boldsymbol{C}_6,\ \boldsymbol{C}_{3h}(\boldsymbol{C}_3),\ \boldsymbol{C}_{6h}(\boldsymbol{C}_6)$	$4,\ \bar{4}',\ 4/m'$ $3,\ \bar{3}'$ $6,\ \bar{6}',\ 6/m'$	$\begin{bmatrix} \alpha_{11} & \alpha_{12} & 0 \\ -\alpha_{12} & \alpha_{11} & 0 \\ 0 & 0 & \alpha_{33} \end{bmatrix}$
$\boldsymbol{S}_4$ $\boldsymbol{C}_4(\boldsymbol{C}_2)$ $\boldsymbol{C}_{4h}(\boldsymbol{S}_4)$	$\bar{4}$ $4'$ $4'/m'$	$\begin{bmatrix} \alpha_{11} & \alpha_{12} & 0 \\ \alpha_{12} & -\alpha_{11} & 0 \\ 0 & 0 & 0 \end{bmatrix}$
$\boldsymbol{D}_4,\ \boldsymbol{C}_{4v}(\boldsymbol{C}_4)$ $\boldsymbol{D}_{2d}(\boldsymbol{D}_2),\ \boldsymbol{D}_{4h}(\boldsymbol{D}_4)$ $\boldsymbol{D}_3,\ \boldsymbol{C}_{3v}(\boldsymbol{C}_3),\ \boldsymbol{D}_{3d}(\boldsymbol{D}_3)$ $\boldsymbol{D}_6,\ \boldsymbol{C}_{6v}(\boldsymbol{C}_6)$ $\boldsymbol{D}_{3h}(\boldsymbol{D}_3),\ \boldsymbol{D}_{6h}(\boldsymbol{D}_6)$	$422,\ 4m'm'$ $\bar{4}'2m'\,[\bar{4}'m'2],\ 4/m'm'm'$ $32,\ 3m',\ \bar{3}'m'$ $622,\ 6m'm'$ $\bar{6}'m'2\,[\bar{6}'2m'],\ 6/m'm'm'$	$\begin{bmatrix} \alpha_{11} & 0 & 0 \\ 0 & \alpha_{11} & 0 \\ 0 & 0 & \alpha_{33} \end{bmatrix}$
$\boldsymbol{C}_{4v},\ \boldsymbol{D}_4(\boldsymbol{C}_4)$ $\boldsymbol{D}_{2d}(\boldsymbol{C}_{2v}),\ \boldsymbol{D}_{4h}(\boldsymbol{C}_{4v})$ $\boldsymbol{C}_{3v},\ \boldsymbol{D}_3(\boldsymbol{C}_3),\ \boldsymbol{D}_{3d}(\boldsymbol{C}_{3v})$ $\boldsymbol{C}_{6v},\ \boldsymbol{D}_6(\boldsymbol{C}_6)$ $\boldsymbol{D}_{3h}(\boldsymbol{C}_{3v}),\ \boldsymbol{D}_{6h}(\boldsymbol{C}_{6v})$	$4mm,\ 42'2'$ $\bar{4}'2'm\,[\bar{4}'m2'],\ 4/m'mm$ $3m,\ 32',\ \bar{3}'m$ $6mm,\ 62'2'$ $\bar{6}'m2'\,[\bar{6}'2'm],\ 6/m'mm$	$\begin{bmatrix} 0 & \alpha_{12} & 0 \\ -\alpha_{12} & 0 & 0 \\ 0 & 0 & 0 \end{bmatrix}$
$\boldsymbol{D}_{2d},\ \boldsymbol{D}_{2d}(\boldsymbol{S}_4)$ $\boldsymbol{D}_4(\boldsymbol{D}_2),\ \boldsymbol{C}_{4v}(\boldsymbol{C}_{2v})$ $\boldsymbol{D}_{4h}(\boldsymbol{D}_{2d})$	$\bar{4}2m,\ \bar{4}m'2'$ $4'22',\ 4'm'm$ $4'/m'm'm$	$\begin{bmatrix} \alpha_{11} & 0 & 0 \\ 0 & -\alpha_{11} & 0 \\ 0 & 0 & 0 \end{bmatrix}$
$\boldsymbol{T},\ \boldsymbol{T}_h(\boldsymbol{T})$ $\boldsymbol{O},\ \boldsymbol{T}_d(\boldsymbol{T}),\ \boldsymbol{O}_h(\boldsymbol{O})$	$23,\ m'\bar{3}'$ $432,\ \bar{4}'3m',\ m'\bar{3}'m'$	$\begin{bmatrix} \alpha_{11} & 0 & 0 \\ 0 & \alpha_{11} & 0 \\ 0 & 0 & \alpha_{11} \end{bmatrix}$

1.5.8. Magnetoelectric effect

Curie (1894) stated that materials that develop an electric polarization in a magnetic field or a magnetization in an electric field may exist. This prediction was given a more precise form by Landau & Lifshitz (1957), who considered the invariants in the expansion of the thermodynamic potential up to linear terms in H_i. For materials belonging to certain magnetic point groups, the thermodynamic potential Φ can be written in the form

$$\Phi = \Phi_0 - \alpha_{ij} E_i H_j. \qquad (1.5.8.1)$$

If (in the absence of a magnetic field) an electric field $\mathbf{E}$ is applied to a crystal with potential (1.5.8.1), a magnetization will be produced:

$$\mu_0^* M_j = -\frac{\partial \Phi}{\partial H_j} = \alpha_{ij} E_i. \qquad (1.5.8.2)$$

Conversely, an electric polarization $\mathbf{P}$ arises at zero electric field if a magnetic field is applied:

$$P_i = -\frac{\partial \Phi}{\partial E_i} = \alpha_{ij} H_j. \qquad (1.5.8.3)$$

This phenomenon is called the magnetoelectric effect. A distinction is made between the linear magnetoelectric effect described above and two types of bilinear magnetoelectric effects. These bilinear effects arise if the thermodynamic potential contains terms of the form $E_i H_j H_k$ or $H_i E_j E_k$. They will be described in Section 1.5.8.2.